New Device for Controlling Asymmetric Flowfields on Forebodies at Large Alpha

Cary A. Moskovitz*
North Carolina State University, Raleigh, North Carolina 27695
Robert M. Hall†
NASA Langley Research Center, Hampton, Virginia 23665
and
F. R. DeJarnette‡
North Carolina State University, Raleigh, North Carolina 27695

An exploratory experimental investigation of a new device to control the asymmetric flowfield on forebodies at large angles of attack has been conducted. The device is a rotatable forebody tip, which varies in cross section from circular at its base to elliptic at its tip. The device itself extends over a small portion of the aircraft or missile forebody. The device provides two important improvements. First, it replaces the normally random behavior of the nose side force as a function of nose tip orientation with a predictable and generally sinusoidal distribution; second, the device shows promise for use as part of a vehicle control system to be deflected in a prescribed manner to provide additional directional control for the vehicle. The device was tested on a cone/cylinder model having a 10-deg semiapex angle and on a 3.0-caliber tangent ogive model. Data were taken with each model at a Reynolds number of 8.4×10^4 based on cylinder diameter and by a helium-bubble flow visualization technique at a Reynolds number of 2.4×10^4.

Nomenclature

C_p = pressure coefficient, $(p - p_\infty)q_\infty$
C_y = sectional side-force coefficient, (local side force)/(q_∞ sin$\alpha 2d$)
D = base diameter of body, in.
d = local body diameter, in.
p_∞ = freestream pressure
q_∞ = freestream dynamic pressure
V_∞ = freestream velocity, ft/s
α = angle of attack, deg
β = angle of sideslip, deg
ϕ_m = roll orientation of body, counterclockwise, deg
ϕ_t = roll orientation of tip (ogive model only), counterclockwise, deg

Introduction

THERE is continuing interest in improving the performance of present and future fighters and missiles by increasing their high angle-of-attack capability. Improvements in high angle-of-attack capabilities will require advances in our understanding of the vortical flow physics as well as improvements in wind-tunnel testing procedures. As one aspect of this broad problem area, the vortical flow over aircraft and missile forebodies has been the object of much research[1,2] since vortex asymmetries over a vehicle forebody can lead to very large yawing moments that can overpower a vehicle control system. This research has traditionally focused on 1) determining at what angle of attack the onset of asymmetries occurs and the development of those asymmetries,[1-6] 2) the dependence of side force on the orientation of nominally axisymmetric bodies,[7-9] 3) examining forebody cross section as a passive means of diminishing the effect of the vortex asymmetries,[10,11] and 4) using measures on the forebody to give active directional control power.[12-14] The present report addresses aspects of areas 2, 3, and 4.

The device investigated is a rotatable nose tip that is circular at its base and elliptic at the tip (Fig. 1). The idea of having an elliptically shaped forebody with the major axis horizontal is not new,[10,11] but the present reasoning for its use and its application are unique. The present application came out of a desire to understand the side-force distributions shown by Lamont,[7,8] which were somewhat sinusoidal in nature but had the additional aspect of being double cycle in nature; that is, the curve went through two cycles in 360 deg of rotating the model about its body axis. The most obvious explanation of the double cycle nature of Lamont's side force was that the nose tips had been finished in some manner to give some ellipticity at the nose tips. (Irregularities in tip shape were proposed by Hunt[1] as one of several possible mechanisms respon-

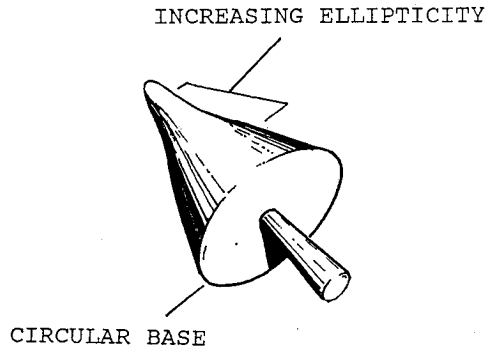

Fig. 1 Sketch of rotatable elliptical tip.

Received Jan. 20, 1990; revision received Aug. 23, 1990; accepted for publication Aug. 24, 1990.

*Graduate Research Assistant; currently Research Associate, Department of Aerospace and Ocean Engineering, Virginia Polytechnic Institute and State University, Blacksburg, VA.
†Senior Research Engineer. Associate Fellow AIAA.
‡Professor, Mechanical and Aerospace Engineering. Associate Fellow AIAA.

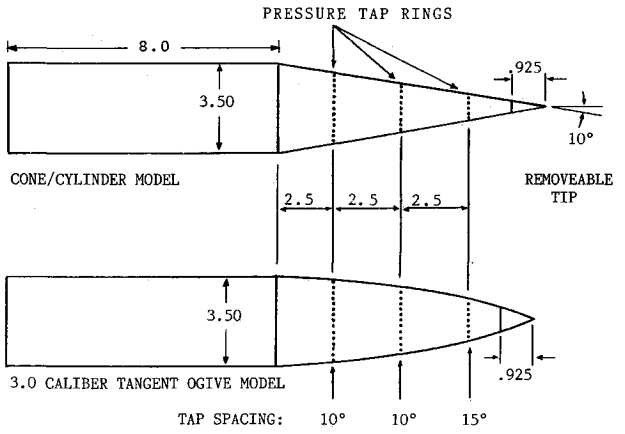

Fig. 2 Sketch of model geometry and pressure tap locations (dimensions in inches).

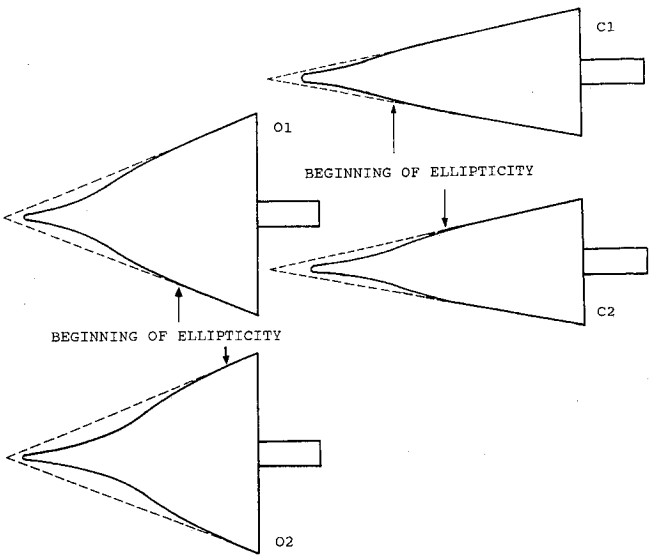

Fig. 3 Sketches of tips for cone and ogive models (dimensions in inches).

sible for determining flowfield asymmetries.) Therefore, a known geometric perturbation was introduced to the model such that it would be the dominant mechanism driving the asymmetry.

Consequently, the present program of examining nose tips that had been purposefully given ellipticity at the apex was originally an attempt to reproduce the two-cycle nature of the Lamont side-force data. As will be demonstrated, this effort succeeded, and using this sort of planned elliptic perturbation near the nose tip may have important implications for wind-tunnel testing technique as well as for a possible active lateral control device.

Equipment and Procedure

The current investigation was conducted in the North Carolina State University subsonic wind tunnel at values of Reynolds numbers corresponding to laminar flow. It is a closed return tunnel having a turbulence factor of 1.2 with a test section 45 in. wide, 32 in. high, and 46 in. long with Plexiglas sides and top, and it is ventilated to room pressure. The sting rotates on a circular arc segment having a 4.0-ft radius and deflects < 0.10 deg at the sting/model junction. The models used were a cone with cylindrical afterbody having a semicone angle of 10 deg and a 3.0-caliber tangent ogive, with dimensions as shown in Fig. 2. Also shown are the locations of the three circumferential rings of pressure taps and the tap angular spacing. Both models had replaceable tips.

Elliptical tips were constructed for each model by filing by hand the foremost section of a slightly blunt tip to the desired shape. Elliptical tips for the cone are C1 and C2, of which the elliptical region of C1 extended further down the tip than did that of C2. For the ogive, tips O1 and O2 were made, where O2 had the larger ellipticity and the elliptical region extended farther down the tip. Sketches of the elliptical tips are shown in Fig. 3. The elliptical cone tips screwed onto the cone model to a fixed position, whereas the ogive tips (O1 and O2) were free to rotate independently of the model and were held in place by a thick silicone grease. Therefore, the roll orientation of the cone tips was controlled by rolling the model, and data will be presented with respect to model roll position ϕ_m. Since the elliptical ogive tips were rolled independently, data associated with O1 and O2 will be presented with respect to tip roll position ϕ_t.

Pressure measurements were performed at a freestream velocity of 45 ft/s corresponding to a Reynolds number of 8.4×10^4 based on cylinder diameter. Pressure tubes from each model were connected to a pair of 48-port Scanivalve transducers and a Hewlett-Packard 9122 computer. Pressure measurements were made for all tips at angles of attack from 30 to 60 deg in 10-deg increments. The tips were rolled through 360 deg in 15-deg increments with an accuracy of ± 2 deg. For the cone, the entire model was rotated, whereas for the ogive, only the tip was rotated. Additional pressure data were taken with ogive tip O2. These included rolling the tip through 180 deg in 5-deg increments at an angle of attack of 60 deg and also rolling the tip through 180 deg in 15-deg increments with the model positioned at sideslip angles of 10 and 15 deg at angles of attack from 40 to 60 deg. The integrated pressures were plotted as a function of model or tip roll position to give the behavior of sectional side force C_y with tip position. The integrated pressures from each row of taps are presented in the figures as different line types corresponding to rows 1, 2, and 3, respectively, from the foremost row.

Flow visualization was performed on flowfields of interest at a velocity of 15 ft/s corresponding to a Reynolds number of 2.5×10^4. As shown in Fig. 4, an arc lamp was placed outside of the test section and directed such that the beam was nearly parallel with the model's upper surface. A wand that emitted

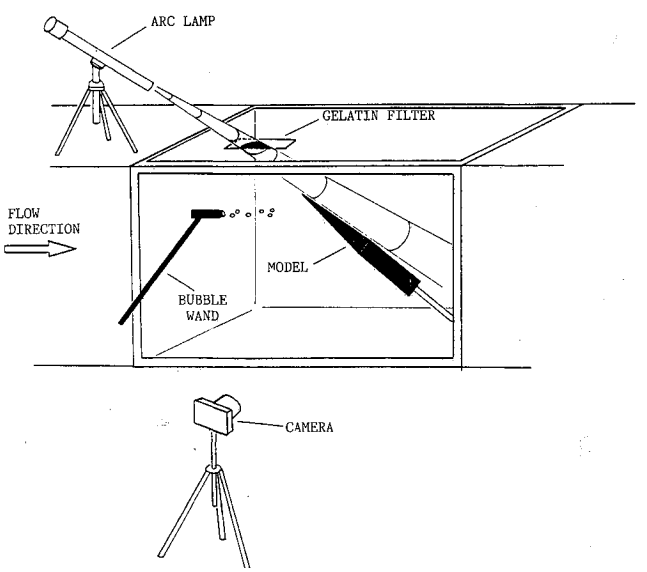

Fig. 4 Schematic of setup for flow visualization: side view.

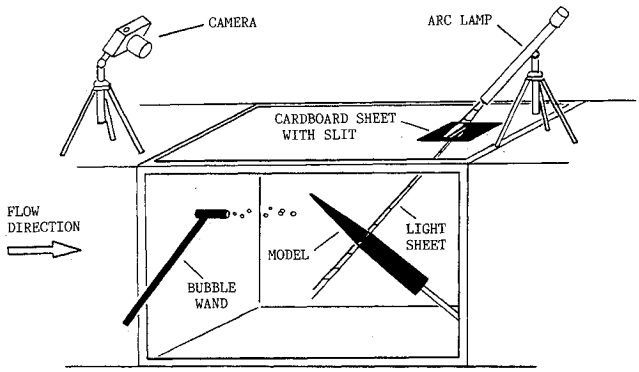

Fig. 5 Schematic of setup for flow visualization: cross section.

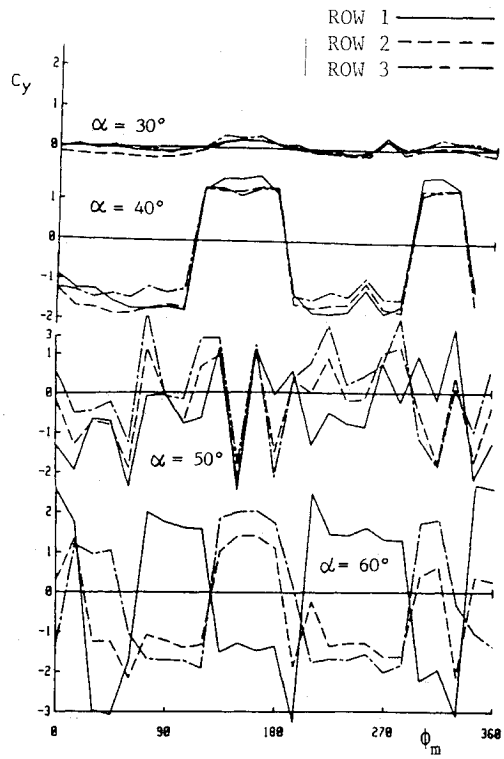

Fig. 6 Variation of sectional side-force coefficient with model roll position: sharp axisymmetric tip on cone model.[3]

neutrally buoyant helium bubbles was held upstream of the model apex. This illuminated the vortices so that side-view photographs showing the model and the vortex trajectories could be taken with a 35-mm camera and a ¾-in. video camera positioned outside of the test section. In order to distinguish between the starboard (closer to the camera) and port (farther from the camera) vortices, pieces of yellow and blue gelatin filters were placed on the Plexiglas test-section top such that the light striking the starboard side of the model was tinted yellow, whereas that on the port side was tinted blue. Cross-section photographs were taken by repositioning the equipment as shown in Fig. 5. The lamp was directed such that the beam was now normal to the model axis with cardboard sheets allowing only a strip of light to cross the model, and the 35-mm camera was placed directly in line with the model axis. The bubble wand was traversed across the test section upstream of the model with the shutter open, a process that took about 10 s on the average. The procedure was performed with the light sheet illuminating vortical crossflow patterns at each of the pressure ring locations.

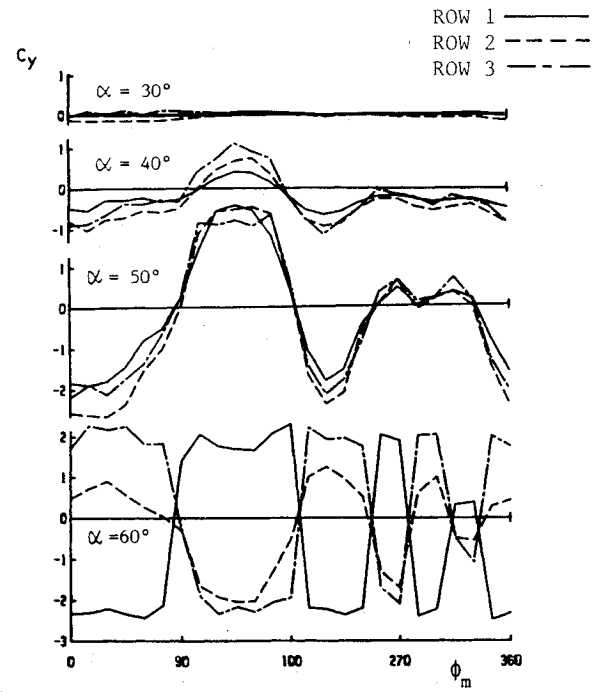

Fig. 7 Variation of sectional side-force coefficient with model roll position: blunt axisymmetric tip on cone model.[3]

Results and Discussion

Cone Model

Since the elliptical tips were made by filing down blunt tips, an accurate assessment of the data must compare the elliptical tips to both sharp and blunt tips. Figures 6 and 7 show the variations of sectional side-force coefficient C_y with model roll position ϕ_m throughout the range of angles of attack tested for a sharp and a blunt tip on the cone model.[3] In Fig. 6, it can be seen that for sharp tips there is little side force at an incidence of 30 deg. At 40 deg, there are significant side forces. Although variations with roll are generally smooth, they do not occur with any regularity. It has been shown[3,4] that these variations are caused by distortion of the tip shape due to machining imperfections. By an angle of attack of 50 deg, vortices had begun to shed from the body. Therefore, three or more vortices were present in the flowfield and consecutive side-force reversals occurred with increasing angle of attack. Figure 7 shows even less side force at α = 30 and 40 deg due to the blunter tip. Again, there is no predetermined pattern to the behavior of C_y with roll position. Note that, for the blunt tip, shedding did not begin until after α = 50 deg.

These trends can be compared with those of the elliptical tips (Figs. 8 and 9) for which it can be seen that there are significant side forces at α = 30 deg. This is caused by the abnormally large geometric perturbation at the apex because of the ellipticity. At this moderate angle the magnitude of the side force is sensitive to the size of the perturbation. Consequently, the rotation of the elliptic tip results in the sinusoidal nature of the side-force distribution. At higher angles of attack, the flow becomes increasingly bistable in nature resulting in a more square-wave C_y distribution. The variation with ϕ_m is very well behaved, being nearly sinusoidal with sign changes occurring nearly every 90 deg. Roll positions producing zero side force nearly coincide with the symmetric positions of the tips. That they do not coincide can be attributed to the imperfections in the hand-filed tips and to the limited accuracy with which the tips could be set. The behavior is essentially the same at α = 40 and 50 deg except that the sinusoidal shape gives way to a more square-wave shape. Therefore, making the tip elliptical was indeed successful in producing well-behaved, predictable roll behavior.

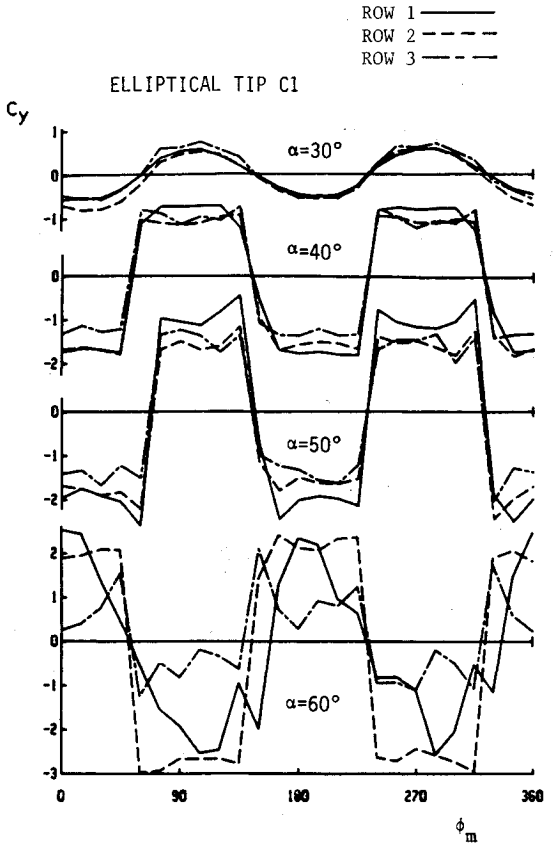

Fig. 8 Variation of sectional side-force coefficient with model roll position: cone tip C1.

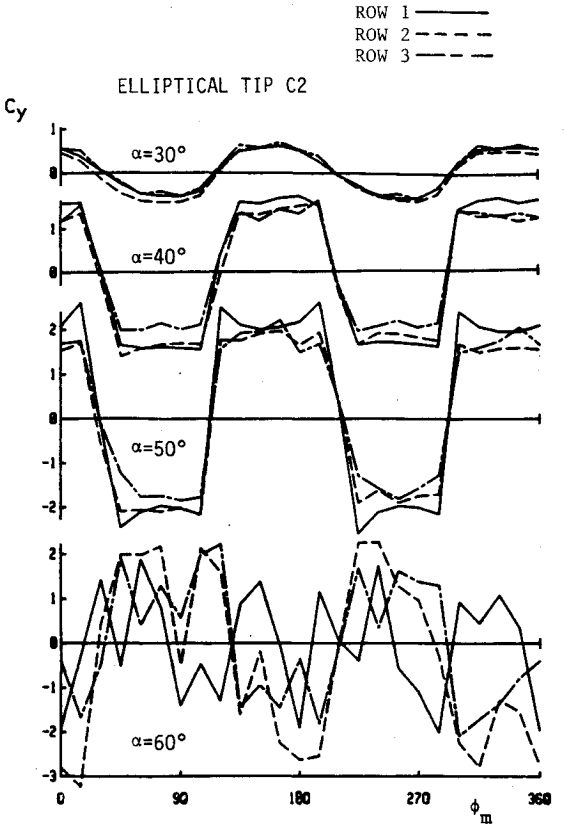

Fig. 9 Variation of sectional side-force coefficient with model roll position: cone tip C2.

Ogive Model

In order to evaluate the rotatable elliptical tip on a forebody shape more representative of an aircraft or missile, two elliptical tips (O1 and O2) were constructed for the ogive model. The tips differed in their ellipticity and the extent to which the elliptic region persisted (axially) down the tip. Again, a comparison of the data from the elliptical tips with similar data from axisymmetric sharp and blunt tips is necessary in order to evaluate the device.

Figures 10 and 11 show the variation of sectional side force with model roll position for typical sharp and blunt tips on the ogive model.[3] As with the cone, there is no particular pattern to the behavior in either case. The only predictable trend is the increase in the maximum side force with increasing angle of attack. Side force distributions for $\alpha = 30$ and 40 deg are essentially flat with the ogive body and are not shown due to space limitations.

In contrast, the data from the elliptical tips (Figs. 12 and 13) show very regular, essentially sinusoidal behavior from 30- to 60-deg angle of attack. Note that throughout this range only the magnitude of the side forces changed and that significant, predictable side forces were possible at an angle of attack as low as 40 deg. Flow visualization photographs showing the vortex core trajectories due to tip O2 at $\alpha = 50$ deg are presented in Fig. 14. The progression from nearly symmetric flow with $\phi_t = 0$ to a state of maximum symmetry at $\phi_t = 45$ deg can be seen. Side-view and cross-section photographs for $\alpha = 60$ deg are shown in Figs. 15a and 15b. Here, the positions of the vortex cores at pressure row 3 can be seen in addition to the vortex trajectories. Note the small but definite asymmetry at the intermediate tip position of $\phi_t = 7.5$ deg in Fig. 15b. The magnitudes of the side forces due to tip O2 are slightly larger than those due to the less elliptical O1. Therefore, the amount of ellipticity may have an effect on the level of side force obtainable.

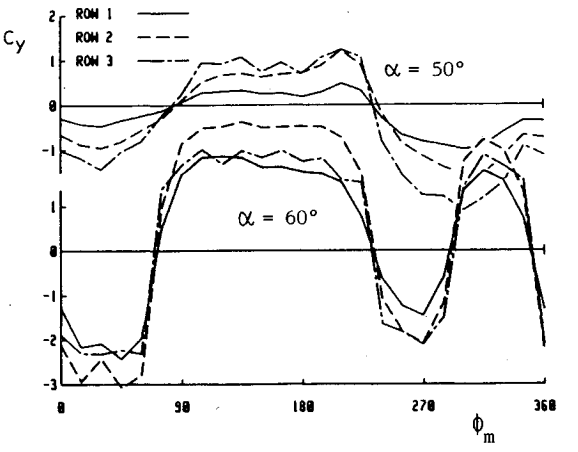

Fig. 10 Variation of sectional side-force coefficient with tip roll position: sharp axisymmetric tip on ogive model.[3]

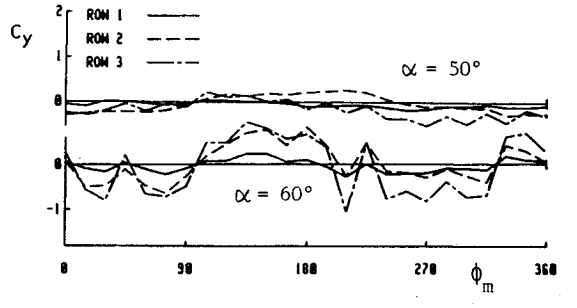

Fig. 11 Variation of sectional side-force coefficient with tip roll position: blunt axisymmetric tip on ogive model.[3]

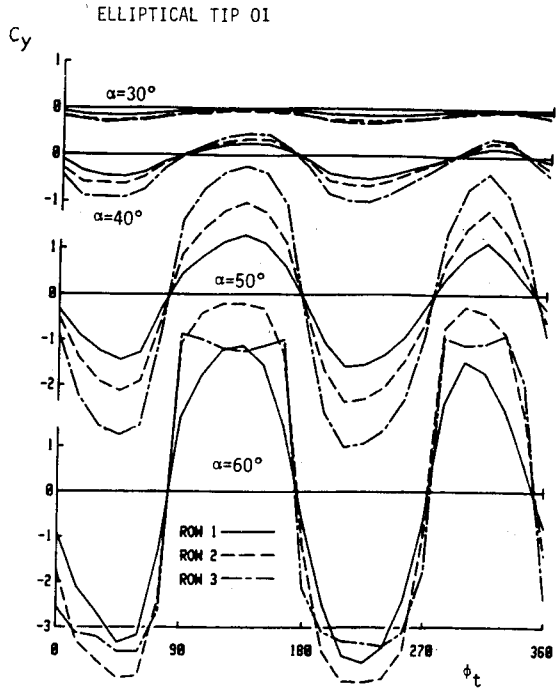

Fig. 12 Variation of sectional side-force coefficient with tip roll position: ogive tip O1.[3]

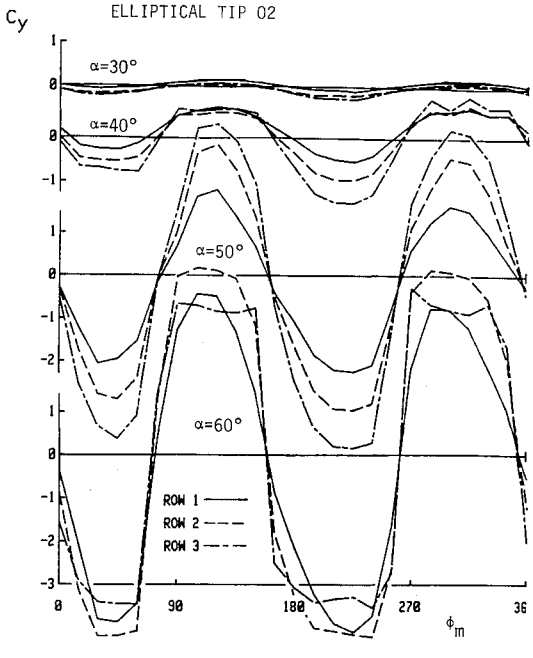

Fig. 13 Variation of sectional side-force coefficient with tip roll position: ogive tip O2.[3]

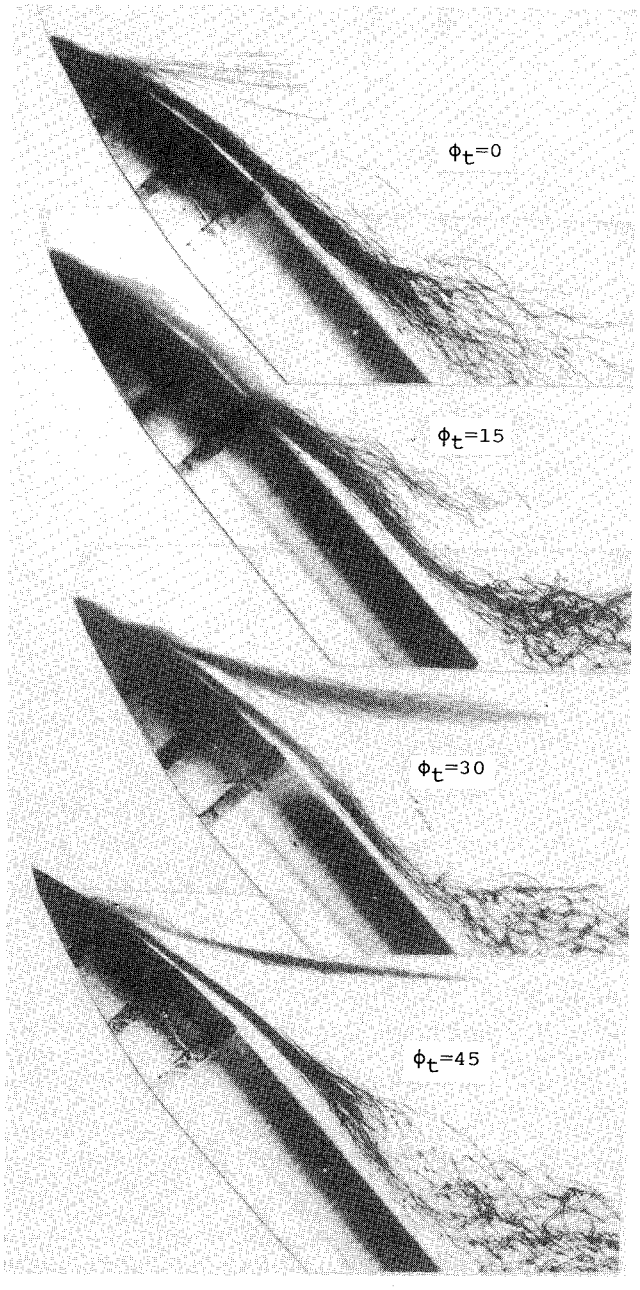

Fig. 14 Side-view flow visualization for ogive tip O2 at α = 50 deg.

Controllability

In order to determine the effectiveness of the rotatable tip as a useful aircraft control device, two other factors were tested. First was the effectiveness of the device when the forebody was at nonzero sideslip, and second, the ability of the device to produce low levels of side force with small ϕ_t and large side forces with large ϕ_t.

Sideslip tests were conducted with the ogive model and tip O2 at sideslip angles of 10 and 15 deg. The ability of the elliptical tip to produce restoring side forces is determined by the magnitude of the maximum negative C_y, because this is the force in the direction opposite the sideslip. With a sideslip angle of 10 deg, some restoring force was possible throughout the angle-of-attack range tested. The trends were similar for β = 15 deg except that at α = 40 deg the elliptical tip was not quite able to produce a restoring force.

Tests of the elliptical tip with a reduced roll increment of 5 deg were conducted with the ogive model and tip O2 at α = 60 deg. Since the slope of the portion of the C_y curves near C_y = 0 increased with increasing angle of attack, α = 60 deg provided the worst case for obtaining a good control input/force output relationship. As seen in Fig. 16, the variation of side force with 5-deg tip roll increments is smooth. A deflection of ϕ_t of 5 deg from C_y = 0 produces a side force less than half of the maximum with consecutive roll positions producing smaller changes in C_y. Consequently, even at high angles of attack where the usual side force distribution with ϕ_t is considered to be nearly square wave in nature, moderate values of control power are available with small changes in ϕ_t.

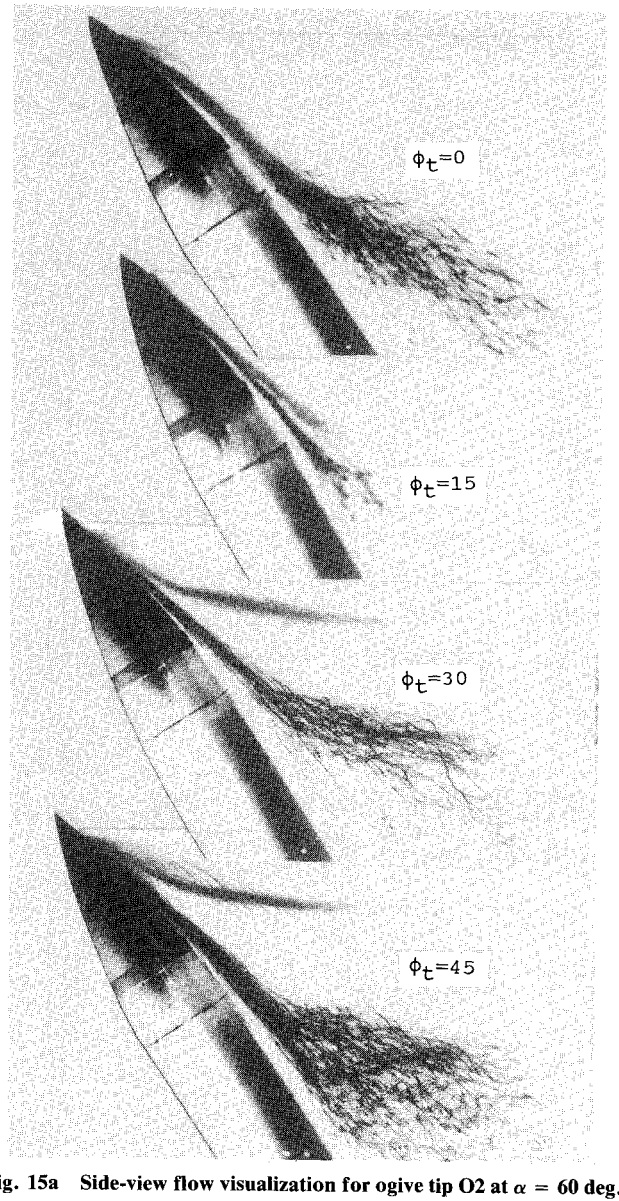

Fig. 15a Side-view flow visualization for ogive tip O2 at α = 60 deg.

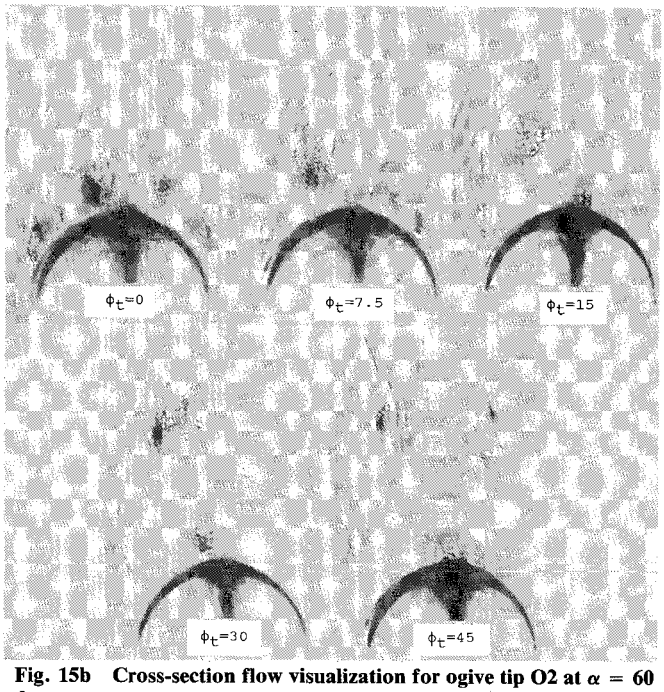

Fig. 15b Cross-section flow visualization for ogive tip O2 at α = 60 deg.

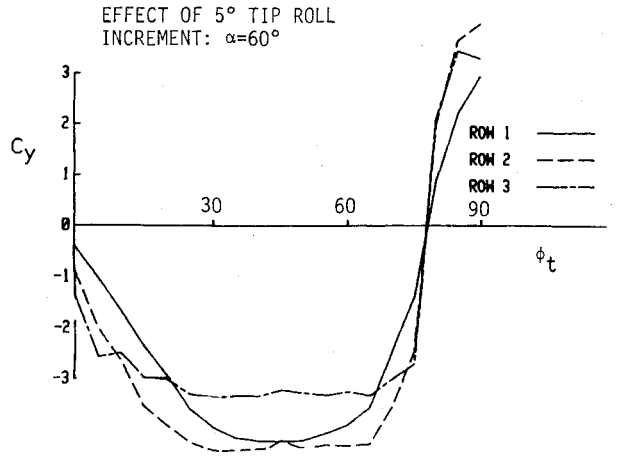

Fig. 16 Variation of sectional side-force coefficient with 5-deg tip roll increment: ogive tip O2 at α = 60 deg.

Conclusions and Recommendations

An experimental investigation has been conducted in order to evaluate a new device to control the asymmetric vortical flow that occurs on slender bodies at large angles of attack. The device is a rotatable tip, elliptic in cross section. The device was tested on a 10-deg cone/cylinder model and a 3.0-caliber tangent ogive model at laminar flow conditions. The following conclusions are drawn from this investigation:

1) By making the tip of a slender-body model elliptic in cross section, regular, predictable, and repeatable behavior of sectional side force with model roll position is achieved. Therefore, the flowfields themselves are regular and predictable.

2) An elliptical tip ensures the availability of a large-amplitude side-force distribution even at moderate angles of attack.

3) The elliptical tip may perform well as an aircraft high angle-of-attack directional control device and warrants further research.

4) The elliptical tip could produce restoring forces at sideslip angles as large as 15 deg and at angles of attack up to 60 deg.

The results from these preliminary, low Reynolds numbers are encouraging, and the authors recommend further testing at Reynolds numbers close to those of flight conditions. Also, based on the success at low Reynolds numbers, it is recommended that this device be considered as a means of stabilizing forebody flows during low-speed tests of slender bodies.

References

[1]Hunt, B. L., "Asymmetric Vortex Forces and Wakes on Slender Bodies," AIAA Paper 82-1336, Aug. 1982.

[2]Ericsson, L. E., and Reding, J. P., "Asymmetric Vortex Shedding from Bodies of Revolution," *Tactical Missile Aerodynamics*, edited by M. J. Hemsch and J. N. Nielsen, Vol. 104, Progress in Astronautics and Aeronautics, AIAA, New York, 1986.

[3]Moskovitz, C. A., Hall, R. M., and DeJarnette, F. R., "Effects of Nose Bluntness, Roughness and Surface Perturbations on the Asymmetric Flow Past Slender Bodies at Large Angles of Attack," AIAA Paper 89-2236, Aug. 1989.

[4]Moskovitz, C. A., Hall, R. M., and DeJarnette, F. R., "Effects of Surface Perturbations on the Asymmetric Vortex Flow Over a Slender Body," AIAA Paper 88-0483, Jan. 1988.

[5]Hall, R. M., "Forebody and Missile Side Forces and the Time Analogy," AIAA Paper 87-0327, Jan. 1987.

[6]Hall, R. M., "Influence of Reynolds Number on Forebody Side Forces for 3.5-Diameter Tangent-Ogive Bodies," AIAA Paper 87-2274, Aug. 1987.

[7]Lamont, P. J., "Pressure Around an Inclined Ogive Cylinder with Laminar, Transitional, or Turbulent Separation," *AIAA Journal*, Vol. 20, No. 11, 1982, pp. 1492–1499.

[8]Lamont, P. J., "The Effect of Reynolds Number on Normal and Side Forces on Ogive-Cylinders at High Incidence," AIAA Paper 85-1799, Jan. 1985.
[9]Dexter, P. C., "A Study of Asymmetric Flow Over Slender Bodies at High Angles of Attack in a Low Turbulence Environment," AIAA Paper 84-0505, Jan. 1984.
[10]Keener, E. R., Chapman, G. T., Cohen, L., and Taleghani, J., "Side Forces on Forebodies at High Angles of Attack and Mach Numbers from 0.1 to 0.7: Two Tangent Ogives, Paraboloid and Cone," NASA TM-X-3438, Feb. 1977.
[11]Edwards, O. R., "Northrop F-5F Shark Nose Development," NASA CR-158936, Oct. 1978.
[12]Skow, A. M., Moore, W. A., and Lorincz, D. J., "Forebody Vortex Blowing—A Novel Control Concept to Enhance Departure/Spin Recovery Characteristics of Fighter and Trainer Aircraft," AGARD CP-262, Sept. 1979.
[13]Murri, D. G., and Rao, D. M., "Exploratory Studies of Actuated Forebody Strakes for Yaw Control at High Angles of Attack," AIAA Paper 87-2557, Aug. 1987.
[14]Rao, D. M., Moskovitz, C. A., and Murri, D. G., "Forebody Vortex Management for Yaw Control at High Angles of Attack," International Congress of Aeronautical Sciences, Paper 86-2.5.2, 1986.